

Error-rejecting quantum computing with solid state spins assisted by low-Q optical microcavities

Tao Li and Fu-Guo Deng*

*Department of Physics, Applied Optics Beijing Area Major Laboratory,
Beijing normal University, Beijing 100875, China*

(Dated: November 3, 2015)

We present an efficient proposal for error-rejecting quantum computing with quantum dots (QD) embedded in single-sided optical microcavities based on the interface between the circularly-polarized photon and the QDs. A unity fidelity of the quantum entangling gate (EG) can be implemented with a detectable error that leads to a recycling EG procedure, which improves further the efficiency of our proposal for EG along with robustness to the errors involved in the imperfect input-output process. Meanwhile, we discuss the performance of our proposal for EG on two solid state spins with currently achieved experiment parameters, showing that it is feasible with current experimental technology. It provides a promising building block for solid-state quantum computing and quantum networks.

PACS numbers: 03.67.Lx, 03.67.Pp, 03.67.Bg, 03.67.Hk

I. INTRODUCTION

Compared with the traditional computer, quantum computing [1] can factor an n -bit integer with the magical Shor's algorithm [2], exponentially faster than the best known classical algorithms. It can also run the famous quantum search algorithm, the Grover's algorithm [3] or the optimal Long's algorithm [4], for unsorted database search, which requires $O(\sqrt{N})$ operations only, much faster than the classical one. Both the circuit-based quantum computing and the measurement-based one require quantum entangling gates. That is, the ability to entangle the quantum bits (qubits) is an essential building block in the construction of a quantum computer [1]. Since the early quantum entangling gates for single atoms were designed with the assistance of a high-Q optical cavity [5], more and more attention has been paid to the entangling operation between stationary qubits [6–19].

The entangling gate (EG) between two qubits in previous proposals can be completed by either the coherent control of the direct qubit-qubit interaction or the indirect interaction mediated with high-Q optical cavities. The typical absence of a heralding measurement in this type of EG will lead to some ambiguous error referring to the small photon loss, i.e., the weak excitation of the cavity or the stationary dipole. Some error corrections should be required to achieve the higher fidelity of the EG for making the quantum information processing faithful. These proposals could successfully work under the condition that the amount of noise is less than a small threshold value [20]. Meanwhile, with the increasing error probability, the more additional qubits are needed to complete the fault-tolerant codes, which will increase the complexity of the target quantum system largely [21].

An alternative strategy exploits a measurement on the

auxiliary photonic qubits that entangle with the corresponding stationary qubit to project the target system into an entangled state for obtaining a quantum EG with high fidelity. Its success is heralded by the detection of photons [11–19]. Its fidelity does not suffer from the photon loss noise and it is relatively robust to the variation of the system parameters, while the special schemes involve the optical Bell-state measurement (BSM) assisted by linear optical elements and can success with the maximal efficiency $1/2$ in the ideal situation [22, 23]. Besides the nondeterministic efficiency, the two photons for the BSM are required to be indistinguishable in all degrees of freedom except for the one used to encode the quantum information. Therefore, if the polarization degree of freedom of photons is used to encode the photonic qubit, the perfect control over the arrival time of the photon together with the photonic spectral properties are needed when performing the BSM, which is difficult to achieve at present and even harder outside the laboratory [24].

It is well known that solid state spin systems offer a promising candidate for the realization of quantum computing [25, 26]. Its solid-state nature combined with nano-fabrication techniques provides a relatively simple way to incorporate the spins into optical microcavities, and allows for the generation of arrays of solid qubits [27–29]. One attractive type of the solid state spin system is the electron spin in quantum dot (QD) [29–31]. Not only does it provide ease ways of optical initialization, single qubit manipulation, and readout, but also it processes a long coherence time of the electron spin in QDs which is around several microseconds using spin echo techniques [32–35]. The most existing quantum computing schemes based on single photons and single spins in QDs are performed in a strong coupling regime as a result of cavity quantum electrodynamics (QED) [29, 36–39]. However, the strong coupling regime remains challenge, and some EG proposals for QDs in a low-Q cavity are proposed with decrease in the fidelity and the efficiency of the performance [40–44]. Meanwhile, the solid state spins used

*Corresponding author: fgdeng@bnu.edu.cn

in the quantum computing are supposed to be homogeneous, and the inhomogeneity of the spins will further decrease the feasibility of the proposed solid state spin quantum computing [25].

In this article, we propose a robust proposal for the quantum entangling gate, or EG, between two quantum dots (QDs) embedded in single-sided microcavities [36]. It is a practical proposal for efficient solid quantum computing that overcomes the existing limitations, since the fidelity of the EG for two QDs is always unity and the efficiency of the EG can, in principle, also approach unity. Compared with previous methods based on QDs [37, 40, 43, 44], the present scheme also has several other advantages. First, it does not require the strong coupling limit and can work efficiently in low-Q cavities or even in the regime of resonance scattering where the modified spontaneous emission parameter of QDs coupled resonantly to a microcavity is matched to that in bulk dielectric. Second, the success of our quantum EG between two QDs is heralded with unity fidelity, and it is signaled by the detection of a horizontal polarized photon as a result of cavity QED involving only one effective input-output procedure. Third, the imperfect reflection of the cavity due to deviation from the ideal conditions, i.e., the nonzero photonic bandwidth, the finite coupling rate between the QD and cavity mode, and the mismatch between the incident photon and the cavity mode, will lead to a click on either vertical detectors other than a decrease in the fidelity of the EG. Meanwhile, the states of the QD's subsystem remained are the same as the original ones, and we can input another probe photon to restart the EG directly without any reparation of the QDs, which makes our quantum computing more efficient than others. With our EGs, one can implement universal quantum computing, including the one-way quantum computing and the circuit one.

II. ERROR-REJECTING ENTANGLING GATE FOR TWO QDS IN LOW-Q OPTICAL MICROCAVITIES

Let us consider a quantum system consisting of a single electron charged self-assembled In(Ga)As QD embedded in a single-sided micropillar cavity constructed by two asymmetric distributed Bragg reflectors (DBR) [28, 36–38]. The DBR is fabricated by epitaxial growth of alternating layers, e.g., GaAs and Al(Ga)As, of a quarter-wave thickness and its reflectivity can be well controlled by the number of layers to constitute the single-sided cavity shown in Fig. 1(a). The quantization axis z is chosen along the growth direction and is also parallel to the light propagation direction. The dipole transition associated with the negatively charged QD is strictly governed by Pauli's exclusion principle [45], shown in Fig. 1(b). The single electron ground states have $J_z = \pm 1/2$, denoted $|\uparrow\rangle$ and $|\downarrow\rangle$, respectively, and the optical excited states are the trion states ($X^- = \{|\uparrow\downarrow\uparrow\rangle \text{ or } |\uparrow\downarrow\downarrow\rangle\}$) consist-

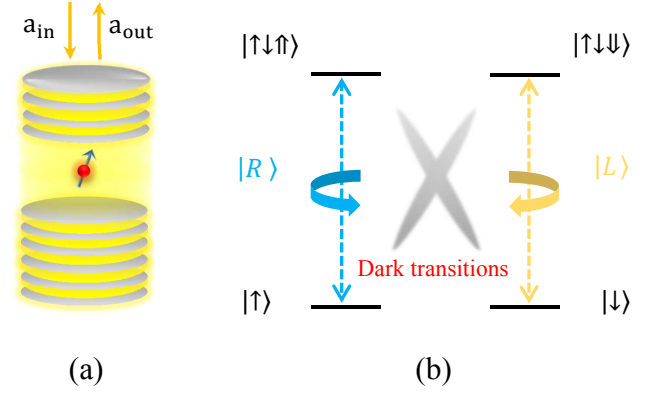


FIG. 1: The spin-dependent transitions for negatively charged exciton X^- . (a) A singly charged QD inside a single-sided optical micropillar cavity. (b) The relative energy levels and the optical transitions of a QD.

ing of two antisymmetric electrons in the singlet state $1/\sqrt{2}(|\uparrow\downarrow\rangle - |\downarrow\uparrow\rangle)$ and one hole with $J_z = \pm 3/2$ ($|\uparrow\rangle$ and $|\downarrow\rangle$). The dipole allowed transitions between the electron state and the trion state are $|\uparrow\rangle \leftrightarrow |\uparrow\downarrow\uparrow\rangle$ and $|\downarrow\rangle \leftrightarrow |\uparrow\downarrow\downarrow\rangle$, along with the absorption of a right-handed circularly polarized photon $|R\rangle$ and a left-handed one $|L\rangle$, respectively, and the crossing transitions are dipole-forbidden [45].

When a circularly polarized probe photon is launched into the single-sided cavity, it will be reflected by the cavity with a spin-dependent reflection coefficient $r_j(\omega)$ [28, 36–38]. The whole process can be represented by Heisenberg equations for the cavity field operator \hat{a} and dipole operator $\hat{\sigma}_-$ in the interaction picture [46],

$$\begin{aligned} \frac{d\hat{a}}{dt} &= -[i(\omega_c - \omega) + \frac{\kappa}{2} + \frac{\kappa_s}{2}]\hat{a} - g\hat{\sigma}_- - \sqrt{\kappa}\hat{a}_{in} + \hat{R}, \\ \frac{d\hat{\sigma}_-}{dt} &= -[i(\omega_{X^-} - \omega) + \frac{\gamma}{2}]\hat{\sigma}_- - g\hat{\sigma}_z\hat{a} + \hat{N}, \end{aligned} \quad (1)$$

where ω_{X^-} , ω_c , and ω are the frequencies of the QD transition, the cavity resonance, and the probe photon, respectively. \hat{R} and \hat{N} are noise operators which help to preserve the desired commutation relations. The parameter g is the coupling strength between X^- and the cavity mode. κ describes the coupling to the input and output ports, while κ_s and γ represent the cavity leakage rate and the trion X^- decay rate, respectively. In the weak excitation limit where the QD dominantly occupies the ground state, assisted by the standard cavity input-output theory $\hat{a}_{out} = \hat{a}_{in} + \sqrt{\kappa}\hat{a}$ [46], one can obtain the spin-dependent reflection coefficient [36, 37, 47]:

$$r_j(\omega) = 1 - \frac{\kappa[i(\omega_{X^-} - \omega) + \frac{\gamma}{2}]}{[i(\omega_{X^-} - \omega) + \frac{\gamma}{2}][i(\omega_c - \omega) + \frac{\kappa}{2} + \frac{\kappa_s}{2}] + jg^2}. \quad (2)$$

Here the subscript j is used to discriminate the cases that the polarized probe photon agrees with the trion

transition ($j = 1$) and feels a QD-cavity coupled system, and that the polarized photon decouples from the trion transition ($j = 0$) and feels an empty cavity.

Suppose the electron spin s of QD is initialized to $|\psi_s\rangle = \alpha|\uparrow\rangle_s + \beta|\downarrow\rangle_s$, with $|\alpha|^2 + |\beta|^2 = 1$. When the input photon is in the polarized state $|\psi_p\rangle = \frac{1}{\sqrt{2}}(|R\rangle - |L\rangle)_p$, the photon reflected by the cavity directly due to the mismatch between the incident probe photonic field and the cavity mode, or reflected by the desired cavity-QD system, together with the QD, evolves into an unnormalized state

$$|\Phi\rangle_H = \frac{\eta_{in}}{\sqrt{2}}[(r_1 \times \alpha|\uparrow\rangle_s + r_0 \times \beta|\downarrow\rangle_s) \otimes |R\rangle_p - (r_0 \times \alpha|\uparrow\rangle_s + r_1 \times \beta|\downarrow\rangle_s) \otimes |L\rangle_p] + \sqrt{1 - \eta_{in}^2}|\psi_s\rangle \otimes |\psi_p\rangle \quad (3)$$

Here η_{in} is the probability amplitude of the photon reflected by the desired cavity-QD system [48]. If one rewrites $|\Phi\rangle_H$ with the linear-polarization basis $\{|H\rangle \equiv \frac{1}{\sqrt{2}}(|R\rangle + |L\rangle), |V\rangle \equiv \frac{1}{\sqrt{2}}(|R\rangle - |L\rangle)\}$, one can get the system composed of the photon p and the electron spin s evolving into a partially entangled hybrid state,

$$|\Phi\rangle_{H0} = \left[\frac{\eta_{in}}{2}(r_1 + r_0) + \sqrt{1 - \eta_{in}^2} \right] (\alpha|\uparrow\rangle_s + \beta|\downarrow\rangle_s) \otimes |V\rangle_p + \frac{\eta_{in}(r_1 - r_0)}{2} (\alpha|\uparrow\rangle_s - \beta|\downarrow\rangle_s) \otimes |H\rangle_p. \quad (4)$$

Here the photon p is partially entangled with the electron spin s . The detection of an $|H\rangle_p$ photon leads to a phase-flip operation on s . Alternatively, the detection of a $|V\rangle_p$ photon signals an error and results in an unchanged electron spin s , no matter the error originates from the mismatch between the incident field and the cavity mode, the low-Q cavity or the detuning. For simplicity, we can take $\eta_{in} \equiv 1$ below, and it will not affect the dominant performance of our EG protocol. Meanwhile, the output state of combined hybrid system composed of the spin s and the probe photon p only depends on the combined coefficients $r_1 - r_0$ or $r_1 + r_0$ of the cavity-QD system, and the output states of two individual inhomogeneous electron spins embedded in different optical microcavities along with their respective probe photons could be amended to be the same by utilizing an adjustable beam splitter. Thus, the inhomogeneity of the solid state spins could be eliminated formally and leads to the homogeneity of the cavity-QD systems.

With the faithful process described above, we can construct an error-rejecting EG, shown in Fig.2, for two identical electron spins s_1 and s_2 (the reflection coefficients $r_i^a = 1$ of the adjustable beam splitter BS_i^a are adopted), which will collapse spins s_1 and s_2 into a state with a deterministic parity after the entangling process. Suppose the electron spin s_i ($i = 1, 2$) is initially in the state $|\Phi\rangle_{s_i} = \alpha_i|\uparrow\rangle_{s_i} + \beta_i|\downarrow\rangle_{s_i}$ with $|\alpha_i|^2 + |\beta_i|^2 = 1$. One probe photon p in the state $|\Phi\rangle_p = \frac{1}{\sqrt{2}}(|R\rangle - |L\rangle)_p$ launched into the import of the EG passes through the beam splitter (BS_1) and will be reflected by either the left cavity

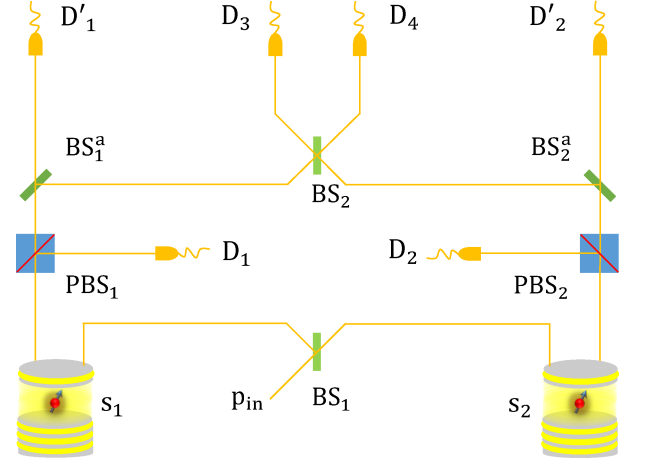


FIG. 2: The schematic setup of the EG. BS represents a 50/50 beam splitter. PBS is the polarizing beam splitter that transmits $|H\rangle$ photons and reflects $|V\rangle$ photons. BS_i^a denotes the beam splitter with adjustable reflection coefficient r_i^a , i.e., $r_1^a = r_2^a = 1$ is utilized for two identical cavity-QD systems; otherwise, $|r_1^a \cdot r_2^a| < 1$ that might lead to the click of single-photon detector D'_i and restart the recycling procedure before a phase-flip operation on spin s_i .

containing the electron spin s_1 or the right one containing s_2 . The unnormalized state of the hybrid system composed of the photon p and the electron spins s_1 and s_2 after reflected by the cavities evolves into

$$|\Phi\rangle_{H1} = \frac{1}{2} \left\{ (r_1 + r_0)(\alpha_1|\uparrow\rangle_{s_1} + \beta_1|\downarrow\rangle_{s_1})(\alpha_2|\uparrow\rangle_{s_2} + \beta_2|\downarrow\rangle_{s_2})(|V\rangle_{p1} + |V\rangle_{p2}) + (r_1 - r_0)[(\alpha_1|\uparrow\rangle_{s_1} - \beta_1|\downarrow\rangle_{s_1})(\alpha_2|\uparrow\rangle_{s_2} + \beta_2|\downarrow\rangle_{s_2})|H\rangle_{p1} + (\alpha_1|\uparrow\rangle_{s_1} + \beta_1|\downarrow\rangle_{s_1})(\alpha_2|\uparrow\rangle_{s_2} - \beta_2|\downarrow\rangle_{s_2})|H\rangle_{p2}] \right\}. \quad (5)$$

Here the subscripts p_1 and p_2 denote photon components that occupy the left path and the right path, respectively. When the photon is in the horizontal polarized state $|H\rangle_{p1}$ or $|H\rangle_{p2}$, the two different spatial modes of photon p are combined on the BS_2 . The interference of $|H\rangle_{p1}$ and $|H\rangle_{p2}$ will collapse the hybrid system into

$$|\Phi\rangle_{H2} = \frac{1}{2}(r_1 - r_0)[(\alpha_1\alpha_2|\uparrow\rangle_{s_1}|\uparrow\rangle_{s_2} - \beta_1\beta_2|\downarrow\rangle_{s_1}|\downarrow\rangle_{s_2})|H\rangle_{p3} + (\alpha_1\beta_2|\uparrow\rangle_{s_1}|\downarrow\rangle_{s_2} - \beta_1\alpha_2|\downarrow\rangle_{s_1}|\uparrow\rangle_{s_2})|H\rangle_{p4}]. \quad (6)$$

Upon the click of the detector D_3 or D_4 , the EG is completed and the electron-spin system s_1s_2 is projected into a subspace with a deterministic parity. In detail, when the photon detector D_3 is triggered on, the spins s_1s_2 collapses into the even parity entangled state of the form

$$|\Phi\rangle_E = \alpha_1\alpha_2|\uparrow\rangle_{s_1}|\uparrow\rangle_{s_2} - \beta_1\beta_2|\downarrow\rangle_{s_1}|\downarrow\rangle_{s_2}. \quad (7)$$

When the detector D_4 clicks, the spins $s_1 s_2$ are projected into the odd parity entangled state of the following form

$$|\Phi\rangle_O = \alpha_1 \beta_2 |\uparrow\rangle_{s_1} |\downarrow\rangle_{s_2} - \beta_1 \alpha_2 |\downarrow\rangle_{s_1} |\uparrow\rangle_{s_2}. \quad (8)$$

Both states $|\Phi\rangle_E$ and $|\Phi\rangle_O$ keep the information of the initial state. The coefficient α_i and β_j could be the states of the other QD spins entangled with s_1 and s_2 , which makes the EG efficient for constructing cluster states. The total probability that either D_3 or D_4 detects one horizontal polarized photon is η_H ,

$$\eta_H = \frac{|r_1 - r_0|^2}{4}. \quad (9)$$

Here η_H equals the efficiency of the EG without recycling procedure.

The first term on the right-hand side of Eq. (5) containing the vertical polarized component $|V\rangle_{p_1}$ ($|V\rangle_{p_2}$) will lead to a click on the photon detector D_1 (D_2). In this time, the state of the electron spins $s_1 s_2$ is projected into $|\Phi\rangle_{s_1} \otimes |\Phi\rangle_{s_2}$, exactly identical to the original one without the interaction between the spins and the photon p , which takes place with the probability η_V ,

$$\eta_V = \frac{|r_1 + r_0|^2}{4}. \quad (10)$$

Here η_V equals the heralded error efficiency of the EG, and the remaining electron spins $s_1 s_2$ could be used in the recycle EG procedure.

In a word, one can obtain two kinds of results with our EG setup. When one probe photon only is exploited, the success or failure of the EG with probabilities η_H or η_V can be heralded, respectively. When the heralded error of EG takes place, a $|V\rangle$ polarized photon is detected and the state of the spin subsystem has not been changed. One can input another probe photon p' in state $|\Phi\rangle_{p'} = \frac{1}{\sqrt{2}}(|R\rangle_{p'} - |L\rangle_{p'})$ to repeat the EG process until a horizontal photon $|H\rangle$ is detected by D_3 or D_4 . This procedure will project the spin system $s_1 s_2$ into an even-parity subspace or an odd-parity one eventually. By taking the recycling procedure into account, the total success probability η_S of our error-rejecting EG is

$$\eta_S = \frac{|r_1 - r_0|^2}{4 - |r_1 + r_0|^2}, \quad (11)$$

which is state-independent, resulting in a more efficient quantum computing.

III. CLUSTER STATE GENERATION WITH OUR EG FOR MEASUREMENT BASED ONE-WAY QUANTUM COMPUTATION

Our error-rejecting EG can be used directly to implement the one-way quantum computing [25, 49, 50] based on QDs embedded in optical cavities. In the following, we demonstrate that our EG can be used to construct the

two-dimensional (2D) QD cluster state [25, 51, 52], which constitutes the base of one-way quantum computing on solid state spins.

Suppose there are $j+1$ QD electron spins $\{s_1, s_2, \dots, s_j\}$ and s_{j+1} , and s_{j+1} is initialized to be the state $\frac{1}{\sqrt{2}}(|\uparrow\rangle_{j+1} - |\downarrow\rangle_{j+1})$ and the first j spins are initially in the 1D cluster state of the form

$$|\psi_j\rangle = (|\uparrow\rangle_1 + |\downarrow\rangle_1 \hat{Z}_2)(|\uparrow\rangle_2 + |\downarrow\rangle_2 \hat{Z}_3) \cdots (|\uparrow\rangle_j + |\downarrow\rangle_j), \quad (12)$$

with the phase flip operator $\hat{Z}_i = |\uparrow\rangle_i \langle \uparrow| - |\downarrow\rangle_i \langle \downarrow|$. To increase the length of the 1D cluster state, an error-rejecting EG for spins s_j and s_{j+1} is applied. When the EG fails, the state of spin s_j is ambiguous and a state measurement on s_j with basis $\{|\uparrow\rangle, |\downarrow\rangle\}$ will collapse the remaining spins into 1D cluster state of $j-1$ qubits, with or without a \hat{Z}_{j-1} feedback operation. When the EG succeeds by the click of photon detector D_3 , the $j+1$ spins will be projected into

$$|\psi'_{j+1}\rangle = (|\uparrow\rangle_1 + |\downarrow\rangle_1 \hat{Z}_2)(|\uparrow\rangle_2 + |\downarrow\rangle_2 \hat{Z}_3) \cdots (|\uparrow\rangle_j + |\downarrow\rangle_j \hat{Z}_{j+1}), \quad (13)$$

which could be transformed into the 1D cluster state similar to that in Eq. (12) of length $j+1$ by a Hadamard operation \hat{H}_j (\hat{H} completes the following transformation: $|\uparrow\rangle \rightarrow \frac{1}{\sqrt{2}}(|\uparrow\rangle + |\downarrow\rangle)$ and $|\downarrow\rangle \rightarrow \frac{1}{\sqrt{2}}(|\uparrow\rangle - |\downarrow\rangle)$) performed on spin j . If the success of the EG for s_j and s_{j+1} is signaled by the click of D_4 , a local operation $\hat{H}_{j+1} \hat{X}_{j+1}$ (here the spin-flip operator $\hat{X} = |\uparrow\rangle \langle \downarrow| + |\downarrow\rangle \langle \uparrow|$) on spin s_{j+1} could also evolve the $j+1$ spins into the desired 1D cluster state.

This procedure of cluster growth above could be used to generate larger cluster, since the efficiency of our error-rejecting EG $\eta_S > 0.5$ and can, in principle, approach unity. To speed up the cluster generation process, some shorter clusters could be prepared in parallel and then be connected together to generate the longer one [23, 53, 54]. In the following, we will introduce an efficient cluster connecting proposal. Suppose the two 1D clusters M and N available are, respectively, of lengths m and n ,

$$|\psi_m\rangle = (|\uparrow_M\rangle_1 + |\downarrow_M\rangle_1 \hat{Z}_{M_2})(|\uparrow_M\rangle_2 + |\downarrow_M\rangle_2 \hat{Z}_{M_3}) \otimes \cdots (|\uparrow_M\rangle_m + |\downarrow_M\rangle_m), \quad (14)$$

$$|\psi_n\rangle = (|\uparrow_N\rangle_1 + |\downarrow_N\rangle_1 \hat{Z}_{N_2})(|\uparrow_N\rangle_2 + |\downarrow_N\rangle_2 \hat{Z}_{N_3}) \otimes \cdots (|\uparrow_N\rangle_n + |\downarrow_N\rangle_n). \quad (15)$$

Before performing EG on M_m and N_1 , a phase-flip operation \hat{Z}_{M_m} is applied on spin M_m . The success of the EG heralded by the click of photon detector D_3 will project the entire spin system into

$$|\psi_m^n\rangle = (|\uparrow_M\rangle_1 + |\downarrow_M\rangle_1 \hat{Z}_{M_2})(|\uparrow_M\rangle_2 + |\downarrow_M\rangle_2 \hat{Z}_{M_3}) \otimes \cdots (|\uparrow_M\rangle_m + |\downarrow_M\rangle_m) |\uparrow_N\rangle_1 + |\downarrow_N\rangle_1 \hat{Z}_{N_2} \otimes (|\uparrow_N\rangle_2 + |\downarrow_N\rangle_2 \hat{Z}_{N_3}) \otimes \cdots (|\uparrow_N\rangle_n + |\downarrow_N\rangle_n). \quad (16)$$

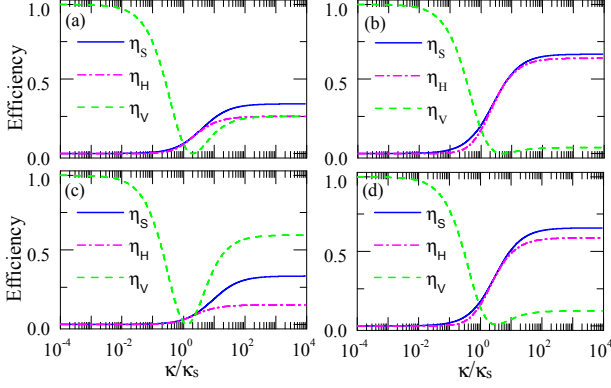


FIG. 3: The efficiency of the EG VS different parameters with $\omega_{X-} = \omega_c$ and $\gamma/\kappa = 0.1$. (a) $\omega_c - \omega = 0$, $C = 1/4$. (b) $\omega_c - \omega = 0$, $C = 1$. (c) $\omega_c - \omega = \gamma$, $C = 1/4$. (d) $\omega_c - \omega = \gamma$, $C = 1$.

An additional Hadamard operation \hat{H} on M_m will evolve the spins system into a 1D cluster $|\psi_{m+n}\rangle$ of $m+n$ qubits. As for the case that the success of the EG is signaled by a click of detector D_4 , a local single qubit operation $\hat{H}\hat{X}$ on M_m can also evolve the spins system into the 1D cluster $|\psi_{m+n}\rangle$.

The cluster connecting procedure generates a 1D cluster of $m+n$ qubit, other than $m+n-1$ in previous schemes [23, 53, 54], since the outcomes of the EG in previous schemes can only lead to an odd parity and the cluster connecting procedure is completed by a spin measurement in the latter. Similar to the previous schemes [23, 53, 54], we can also perform a cross-link between linear chains to construct 2D cluster, which means our EG can be used to complete universal one-way quantum computing efficiently.

IV. PERFORMANCE OF OUR ERROR-REJECTING EG WITH CURRENT EXPERIMENTAL PARAMETERS

The total success probability η_S together with η_H and η_V of our EG are shown in Fig. 3 as a function of the side leakage κ/κ_s with the cooperativity $C = g^2/\gamma\kappa_T$, $\kappa_T \equiv \kappa_s + \kappa$, and $\gamma/\kappa = 0.1$ [55]. We tune the transition frequency ω_{X-} of the QD to be resonant to that of the cavity, $\omega_{X-} = \omega_c$ [56]. When the probe photon is also resonant to cavity, see Fig. 3 (a) and (b), $\eta_S^p = 0.255$ and $\eta_S^r = 0.559$ can be achieved in the regime of resonance scattering $C = 1/4$ and the Purcell regime with $C = 1$, respectively, for $\kappa/\kappa_s = 13$ [44, 57]. When the probe photon detuning from trion transition by γ , shown in Fig. 3 (c) and (d), $\eta_S^p = 0.194$ and $\eta_S^r = 0.538$ can be achieved for the same remaining parameters, and the contribution from the recycling procedure η_V increases. Furthermore, the EG could enjoy a higher efficiency with a lower side leakage but a higher cooperativity C , which can be

achieved by utilizing adiabatic cavities with smaller pillar diameters [55, 57]. In other words, the near unity efficiency of the error-rejecting EG can be achieved when deep Purcell regime with low side leakage is available, and we can easily attribute this improvement of the efficiency to the enhancement of the photon into the cavity mode.

In the above, we can get an ideal error-rejecting EG for QDs with the perfect spin qubit. In fact, the effects of dephasing and decay of the electron spins will affect the performance of the EG. The time needed for the coherent control of single electron spin in QDs is on the scale of picoseconds [32, 33] and the cavity photon time is tens of picoseconds when the cavity Q-factor is about $10^4 - 10^5$ [55]. Meanwhile, the electron spin coherence time of 10 ns has been achieved at zero magnetic field [58], and it could be extended to 2.6 μ s if the all-optical spin echo technique is exploited [34, 35]. The ratio of decoherence time of the spins to the operation time can exceed 10^5 , which suggests the strong promise of electron spin in QDs for scalable quantum computing.

V. DISCUSSION AND CONCLUSION

Our scheme of error-rejecting EG can work efficiently with unity fidelity in the Purcell regime $C > 1/4$ or even the resonantly scattering regime $C = 1/4$. It is robust to the imperfections involved in the practical input-output process, i.e., the nonzero bandwidth, QD or cavity decay, and the finite coupling g/κ , since the fidelity of our EG is unity, independent on the reflective coefficients $r_j(\omega)$, which is far different from other schemes [37, 40, 43, 44]. The original low fidelity or error items originating from the practical input-output process are converted into a relatively lower efficiency in our proposal for EG. Fortunately, the low fidelity or error items will trigger the single-photon detector D_1 or D_2 , which can be used to improve the efficiency of the EG by introducing the recycling procedure. In fact, our recycling procedure can be omitted when perfect circular birefringence is available, since the efficiency η_H of the error-rejecting EG without recycling procedure approaches unity.

The error-rejecting EG only involves one effective input-output process, which makes our scheme more efficient than others since the input-output coupling $\eta_{in} < 1$ [48]. In this situation, the probe photon can be reflected directly by the cavity, and it is harmful and will reduce the fidelity of the entangling process in the other schemes [15, 16, 40, 43, 44]. However, it can only lead to a decrease of the efficiency of our EG, since the photon reflected directly by the microcavity together with the spins will be kept unchanged. In other words, the photon reflected directly by the microcavity is still in $|V\rangle$ polarization and it will trigger the single-photon detector D_1 or D_2 and signal the restarting of the error-rejecting EG. The photon loss during the EG process owing to the inefficiency of the single-photon detector or cavity absorption

will decrease the efficiency of the EG, but it does not affect the fidelity of our EG since both the success of the EG and the restarting of the EG is signaled by a click of the single photon detectors.

In conclusion, we have proposed an efficient error-rejecting EG proposal for two electron spins of QDs embedded in low-Q optical microcavities. With our error-rejecting EGs, a cluster state connection scheme could be completed efficiently. Under the practical experimental condition, the EG could be performed well with the unity fidelity and an efficiency of $\eta_s > 0.5$ for $C = 1$. We believe the EG could provide a promising building block

for solid-state scalable quantum computing and quantum networks in future.

ACKNOWLEDGMENTS

This work is supported by the National Natural Science Foundation of China under Grant No. 11474026 and the Fundamental Research Funds for the Central Universities under Grant No. 2015KJJCA01.

-
- [1] M. A. Nielsen and I. L. Chuang *Quantum Computation and Quantum Information* (Cambridge University Press, Cambridge, UK, 2000).
 - [2] P. W. Shor, SIAM J. Sci. Statist. Comput. **26**, 1484 (1997).
 - [3] L. K. Grover, Phys. Rev. Lett. **79**, 325 (1997).
 - [4] G. L. Long, Phys. Rev. A **64**, 022307 (2001).
 - [5] J. I. Cirac and P. Zoller, Phys. Rev. A **50**, R2799–R2802 (1994).
 - [6] J. I. Cirac, P. Zoller, H. J. Kimble, and H. Mabuchi, Phys. Rev. Lett. **78**, 3221–3224 (1997).
 - [7] M. D. Lukin and P. R. Hemmer, Phys. Rev. Lett. **84**, 2818–2821 (2000).
 - [8] S. B. Zheng and G. C. Guo, Phys. Rev. Lett. **85**, 2392–2395 (2000).
 - [9] E. Hagley, X. Maitre, G. Nogues, C. Wunderlich, M. Brune, J. M. Raimond, and S. Haroche, Phys. Rev. Lett. **79**, 1–5 (1997).
 - [10] J. Borregaard, P. Kmr, E. M. Kessler, A. S. Sørensen, and M. D. Lukin, Phys. Rev. Lett. **114**, 110502 (2015).
 - [11] L. M. Duan, M. Lukin, J. I. Cirac, and P. Zoller, Nature **414**, 413–418 (2001).
 - [12] X. L. Feng, Z. M. Zhang, X. D. Li, S. Q. Gong, and Z. Z. Xu, Phys. Rev. Lett. **90**, 217902 (2003).
 - [13] D. E. Browne, M. B. Plenio, and S. F. Huelga, Phys. Rev. Lett. **91**, 067901 (2003).
 - [14] C. Simon and W. T. M. Irvine, Phys. Rev. Lett. **91**, 110405 (2003).
 - [15] A. S. Sørensen and K. Mølmer, Phys. Rev. Lett. **90**, 127903 (2003).
 - [16] A. S. Sørensen and K. Mølmer, Phys. Rev. Lett. **91**, 097905 (2003).
 - [17] L. Childress, J. M. Taylor, A. S. Sørensen, and M. D. Lukin, Phys. Rev. A **72**, 052330 (2005).
 - [18] L. M. Duan, M. J. Madsen, D. L. Moehring, P. Maunz, R. N. Kohn, and C. Monroe, Phys. Rev. A **73**, 062324 (2006).
 - [19] P. Maunz, S. Olmschenk, D. Hayes, D. N. Matsukevich, L. M. Duan, and C. Monroe, Phys. Rev. Lett. **102**, 250502 (2009).
 - [20] A. M. Steane, Phys. Rev. A **68**, 042322 (2003).
 - [21] A. G. Fowler, M. Mariantoni, J. M. Martinis, and A. N. Cleland, Phys. Rev. A **86**, 032324 (2012).
 - [22] J. W. Pan, C. Simon, Č. Brukner, and A. Zeilinger, Nature **410**, 1067–1070 (2001).
 - [23] S. D. Barrett and P. Kok, Phys. Rev. A **71**, 060310 (2005).
 - [24] N. Kalb, A. Reiserer, S. Ritter, and G. Rempe, Phys. Rev. Lett. **114**, 220501 (2015).
 - [25] S. C. Benjamin, B. W. Lovett, and J. M. Smith, Laser Photon. Rev. **3**, 556C–574 (2009).
 - [26] T. D. Ladd, F. Jelezko, R. Laflamme, Y. Nakamura, C. Monroe, and J. L. O’Brien, Nature **464**, 45–53 (2010).
 - [27] D. Englund, B. Shields, K. Rivoire, F. Hatami, J. Vučković, H. Park, and M. D. Lukin, Nano letters **10**, 3922–3926 (2010).
 - [28] A. B. Young, R. Oulton, C. Y. Hu, A. C. T. Thijssen, C. Schneider, S. Reitzenstein, M. Kamp, S. Höfling, L. Worschech, A. Forchel, and J. G. Rarity, Phys. Rev. A **84**, 011803 (2011).
 - [29] P. Lodahl, S. Mahmoodian, and S. Stobbe, Rev. Mod. Phys. **87**, 347–400 (2015).
 - [30] D. Loss, and D. P. DiVincenzo, Phys. Rev. A **57**, 120–126 (1998).
 - [31] A. Imamoglu, D. D. Awschalom, G. Burkard, D. P. DiVincenzo, D. Loss, M. Sherwin, and A. Small, Phys. Rev. Lett. **83**, 4204–4207 (1999).
 - [32] G. Kristiaan De, P. David, L. M. Peter, and Y. Yoshihisa, Rep. Prog. Phys. **76**, 092501 (2013).
 - [33] J. Berezovsky, M. H. Mikkelsen, N. G. Stoltz, L. A. Coldren, and D. D. Awschalom, Science **320**, 349–352 (2008).
 - [34] D. Press, K. De Greve, P. L. McMahon, T. D. Ladd, B. Friess, C. Schneider, M. Kamp, S. Höfling, A. Forchel, and Y. Yamamoto, Nat. Photon. **4**, 367–370 (2010).
 - [35] K. De Greve, P. L. McMahon, D. Press, T. D. Ladd, D. Bisping, C. Schneider, M. Kamp, L. Worschech, S. Höfling, A. Forchel, and Y. Yamamoto, Nat. Phys. **7**, 872–878 (2011).
 - [36] C. Y. Hu, W. J. Munro, and J. G. Rarity, Phys. Rev. B **78**, 125318 (2008).
 - [37] C. Y. Hu, A. Young, J. L. O’Brien, W. J. Munro, and J. G. Rarity, Phys. Rev. B **78**, 085307 (2008).
 - [38] H. R. Wei and F. G. Deng, Opt. Express. **22**, 593–607 (2014).
 - [39] H. R. Wei and F. G. Deng, Sci. Rep. **4**, 7551 (2014).
 - [40] E. Waks and J. Vuckovic, Phys. Rev. Lett. **96**, 153601 (2006).
 - [41] A. Auffèves-Garnier, C. Simon, J. M. Gérard, and J. P. Poizat, Phys. Rev. A **75**, 053823 (2007).
 - [42] C. Bonato, F. Haupt, S. S. R. Oemrawsingh, J. Gudat, D. Ding, M. P. van Exter, and D. Bouwmeester, Phys.

- Rev. Lett. **104**, 160503 (2010).
- [43] K. Koshino and Y. Matsuzaki, Phys. Rev. A **86**, 020305 (2012).
 - [44] A. B. Young, C. Y. Hu, and J. G. Rarity, Phys. Rev. A **87**, 012332 (2013).
 - [45] R. J. Warburton, Nat. Mater. **12**, 483–493 (2013).
 - [46] D. F. Walls and G. J. Milburn, Quantum Optics (Springer, New York, 2008).
 - [47] E. Waks and J. Vuckovic, Phys. Rev. A **73**, 041803 (2006).
 - [48] V. Loo, L. Lanco, A. Lemaitre, I. Sagnes, O. Krebs, P. Voisin, and P. Senellart, Appl. Phys. Lett. **97**, 241110 (2010).
 - [49] H. J. Briegel and R. Raussendorf, Phys. Rev. Lett. **86**, 910 (2001).
 - [50] R. Raussendorf and H. J. Briegel, Phys. Rev. Lett. **86**, 5188–5191 (2001).
 - [51] Y. S. Weinstein, C. S. Hellberg, and J. Levy, Phys. Rev. A **72**, 020304 (2005).
 - [52] Z. R. Lin, G. P. Guo, T. Tu, F. Y. Zhu, and G. C. Guo, Phys. Rev. Lett. **101**, 230501 (2008).
 - [53] L. M. Duan and R. Raussendorf, Phys. Rev. Lett. **95**, 080503 (2005).
 - [54] L. M. Duan, M. J. Madsen, D. L. Moehring, P. Maunz, R. N. Kohn, and C. Monroe, Phys. Rev. A **73**, 062324 (2006).
 - [55] J. P. Reithmaier, G. Sek, A. Löffler, C. Hofmann, S. Kuhn, S. Reitzenstein, L. V. Keldysh, V. D. Kulakovskii, T. L. Reinecke, and A. Forchel, Nature **432**, 197–200 (2004).
 - [56] J. Gudat, C. Bonato, E. van Nieuwenburg, S. Thon, H. Kim, P. M. Petroff, M. P. van Exter, and D. Bouwmeester, Appl. Phys. Lett. **98**, 121111 (2011).
 - [57] M. Lerner, N. Gregersen, F. Dunzer, S. Reitzenstein, S. Höfling, J. Mørk, L. Worschech, M. Kamp, and A. Forchel, Phys. Rev. Lett. **108**, 057402 (2012).
 - [58] M. H. Mikkelsen, J. Berezovsky, N. G. Stoltz, L. A. Coldren, and D. D. Awschalom, Nat. Phys. **3**, 770–773 (2007).